

Original Article

In vivo growth and responses to treatment of renal cell carcinoma in different environments

Yahya Alhamhoom, Guisheng Zhang, Mingming Gao, Houjian Cai, Dexi Liu

Department of Pharmaceutical and Biomedical Sciences, College of Pharmacy, University of Georgia, Athens, GA 30602, USA

Received December 30, 2016; Accepted January 2, 2017; Epub February 1, 2017; Published February 15, 2017

Abstract: Renal cell carcinoma is the most common type of kidney cancer in adults and is associated with poor prognosis. The hydrodynamic cell delivery technique was employed in this study to establish tumor growth in mouse lung, liver and kidneys. We demonstrate that Renca^{Luc} cells exhibit different growth rates and responses to the cancer treatment of 5-fluorouracil and cytokine gene therapy when growing in different organs. The tumor growth rate was faster in the kidneys compared to that in the lung and liver. The liver is the second-best organ in support of tumor growth. Tumors in the liver and lung respond to 5-fluorouracil treatment but are less responsive in the kidneys. IL-12 gene therapy resulted in whole-body tumor suppression and prolonged animal survival. IFN- β gene therapy was effective in suppressing tumor growth in the liver but not effective for those in the lung and kidneys. These results suggest that kidney cancer cells, once metastasized in different organs, show different growth patterns and respond differently to treatment. Our data also imply that an animal model with multi-organ tumor growth is critical for development of a new strategy for treatment of tumors when metastasis is suspected. At the same time, the results also provide direct evidence in support of the usefulness of the hydrodynamic tail vein injection as a tool for establishment of tumor growth in the lung, liver and kidneys.

Keywords: Kidney cancer, renal cell carcinoma, hydrodynamic delivery, tumor metastasis, cancer treatment, meta-static animal model

Introduction

Kidney cancer remains a major medical problem, with about 63,000 new cases expected in 2016 [1]. Nephrectomy is the first choice for treatment that is often combined with systemic therapy if tumor metastasis is suspected. Studies have shown that approximately 30% of patients who have undergone surgical removal of renal tumor have metastatic spread [2]. The five-year survival rate for patients with distant metastases is 12% [1]. Conventional chemotherapy and radiation therapy do not work well for treatment of kidney cancers, making renal cancer one of the hardest cancers to treat [3-5].

Renal cell carcinoma (RCC) is the most common type of kidney cancer in adults [6]. Recent advances in understanding the molecular mechanisms of RCC pathogenesis have led to FDA approval of several therapies targeting mammalian target of rapamycin (mTOR), vascular

endothelial growth factor (VEGF), and its tyrosine kinase receptors, in addition to previously approved cytokine (IL-2 and IFN- α) therapies [7]. The new therapies improve survival and show better safety profiles compared to conventional cytokine therapy. These newer therapies, however, do not result in the complete eradication that was seen with cytokine therapies [7-9].

Significant efforts have been made in recent years to develop new strategies and better drugs for cancer treatment. In fact, many compounds have been identified and demonstrated excellent antitumor activity *in vitro* or in animals. However, about 95% of antitumor agents selected based on preclinical animal studies failed in clinic [10]. Many reasons can account for this undesirable outcome, including toxicity, low bioavailability, and/or undesirable pharmacokinetics and pharmacodynamics between mice and humans. One factor that we believe critical is the use of improper animal models for

therapeutic evaluation. Instead of using animals with multiple tumor metastases for drug testing, the animals commonly used for drug evaluation carry either subcutaneous or orthotopic tumors, or tumors growing in a single organ, which is different from clinic where tumor has spread to multiple organs [11-13]. It is possible that tumor cells, once metastasized, grow differently in a new environment and would have different responses to the treatment. To test this possibility, we employed a procedure of hydrodynamic delivery to seed RCC cells into the liver, kidneys, and the lung in mice [14]. Tumor growth in these three organs and their responses to the treatment of 5-FU and cytokine gene therapy are characterized. We show that among the three organs, the kidneys and liver are more supportive for tumor growth than the lung. RCC cells growing in the lung and liver are responsive to 5-FU treatment. Conversely, tumor cells in the liver show higher sensitivity to IFN- β gene therapy. These results confirm our prediction that tumors, once metastasized in different organs, need to be considered as a different type of tumor with new properties. Our results also suggest that the procedure of hydrodynamic cell delivery to establish tumor growth in the lung, liver, and kidneys in mice is a vital tool for assessing new strategies for treatment of metastasized tumor in mice.

Materials and methods

Materials

5-fluorouracil with a purity of 99% was purchased from Sigma-Aldrich (St. Louis, MO). The pLIVE® plasmid vector, containing albumin promoter and the kanamycin resistance gene, was purchased from Mirus Bio (Madison, WI). The pCMV-IL-2 and pCMV-mIL-12 were kindly provided by Dr. Shulin Li (The University of Texas MD Anderson Cancer Center, Houston, TX). pUMVC3-mIL-7 was purchased from Aldevron (Fargo, ND). pORF9-mIL-21 and pORF9-mIL-24 were purchased from InvivoGen (San Diego, CA). pCMV6-mIFN- β and pCMV6-mIL-27 were purchased from OriGene (Rockville, MD). The individual mouse cytokine gene: IFN- β (549 bp), IL-2 (509 bp), IL-7 (500 bp), IL-12 (fused p35 and p40 subunits; 2289 bp), IL-21 (440 bp), IL-24 (555 bp), or IL-27 (1975 bp) was subcloned into multiple cloning sites in pLIVE vector. DNA sequencing was used to confirm con-

structed plasmids. Plasmid DNA was prepared using the method of cesium chloride-ethidium bromide gradient centrifugation and kept in saline at -80°C until use. DNA concentration and purity were determined using OD_{260/280} ratio and confirmed by agarose gel electrophoresis.

Preparation of Renca^{Luc} cells

Mouse Renca cells were purchased from ATCC (Manassas, VA). Luciferase gene was cloned into the FUCRW lentiviral vector and expressed under the regulation of human ubiquitin promoter. Lentiviruses were made under the regulation of the biosafety level 2 at the University of Georgia, Athens, GA. Renca^{Luc} cells, a stable cell line expressing the luciferase gene, were generated by lentiviral infection of the Renca cells. Single cell cloning procedure in a 96-well culture plate was performed to obtain a single colony of luciferase-tagged Renca^{Luc} cells. Tumor cells were cultured in DMEM (ATCC, Manassas, VA) with 10% FBS (Atlanta Biologics, Atlanta, GA) and 1% penicillin/streptomycin (Life Technologies, Carlsbad, CA), and maintained at 37°C supplied with 5% CO₂. At 80-90% confluence, the medium was removed and cells were trypsinized with 2.5 ml per petri dish (10 cm in diameter) of trypsin/EDTA solution (0.25% Trypsin, 2.21 mM EDTA; Mediatech, Herndon, VA) at 37°C for 5 min. Cell suspension was mixed with a complete cell culture medium and cells were collected by centrifugation (1,200 rpm for 5 min). Cell pellets were re-suspended and washed twice with serum-free medium, and then passed through a membrane filter with an average pore size of 40 μ m (BD Falcon, Franklin Lakes, NJ). Cell pellets were obtained by centrifugation of tumor cell suspension at 1,200 rpm for 5 min at room temperature, followed by re-suspending cells in a serum-free medium at a desirable concentration determined by a hemocytometer. Standard calibration curve of luciferase activity as a function of number of Renca^{Luc} cells was established using luciferase assay.

Mice and hydrodynamic cell delivery

Female Balb/c (6-8 weeks old, 18-22 g) mice were purchased from Charles River Laboratories (Wilmington, MA) and housed in a pathogen-free environment in the Animal Facility of the University of Georgia. All animal procedures

Environment affects tumor growth and response to treatment

performed were approved by the Institutional Animal Care and Use Committee of the University of Georgia in Athens, Georgia. To generate multi-organ tumor growth, hydrodynamic cell delivery was utilized as previously described [14]. Briefly, 10^6 Renca^{Luc} cells suspended in serum-free medium in a volume equivalent to 9% body weight was injected into the tail vein of a mouse over 5-8 s. To determine tumor growth in different organs, mice were sacrificed at desirable time points after cell injection, organs were collected and tumor load was determined by histochemistry or/and luciferase assay.

Treatment of tumor-bearing mice

For chemotherapy treatment, tumor-bearing mice were randomly divided into control and treatment groups. The treatment group received intraperitoneal injection of 5-FU (20 mg/kg) and the control animals received carrier solution on day 7. Treatment continued every other day for a total of 6 injections. Mice were euthanized 18 days after tumor cell injection. For cytokine gene therapy, plasmids containing cytokine genes including IFN- β , IL-2, IL-7, IL-12, IL-21, IL-24, or IL-27 were hydrodynamically injected into mice 3 days after tumor inoculation [15, 16]. Tumor growth in mice was assessed using *in vivo* bioluminescence imaging at different time points. Mice receiving injection of pLIVE empty vector served as a control.

In vivo bioluminescence imaging

Bioluminescence imaging was performed using IVIS Imaging System (Perkin-Elmer, Akron, OH). Mice were intraperitoneally injected with 200 μ l (150 mg/Kg) of firefly D-luciferin (Perkin-Elmer, Akron, OH) in phosphate buffered saline and anesthetized 2 min later with isoflurane inhalation (Abbott Lab, Irving, TX). Whole body imaging was performed 15 min after D-luciferin injection using 1 min acquisition time (binning 4, F-stop 1, FOV 12.5). The region of the area of interest was manually adjusted. Light intensity was calculated using the Living Image Software (Perkin-Elmer) with a background subtraction and expressed as photons/second/cm²/steradian (p/s/cm²/sr).

Luciferase assay

Tissue samples collected from sacrificed mice were immediately frozen in liquid nitrogen and

kept at -80°C until use. For luciferase assay, 1 ml of the lysis buffer (100 mM Tris-HCl, 2 mM EDTA and 0.1% Triton X-100, pH 7.8) was added to a piece of tissue (~100 mg) and homogenized using a tissue homogenizer (Dremel, Racine, WI). Tissue homogenates were centrifuged for 10 min in a Microfuge (Beckman Coulter, Brea, CA) at 10,000 rpm at 4°C. Protein concentration of the supernatant was determined by the Bradford protein assay and 10 μ l of supernatant was used to determine luciferase activity [15].

Histochemical analyses by hematoxylin and eosin (H&E) staining

Samples from the lung, liver, and kidneys were collected and fixed in 10% neutrally buffered formalin. Fixed tissue samples were dehydrated, embedded in paraffin, and sectioned at 6 μ m in thickness. Tissue sections were incubated in xylene and stained with H&E following manufacturer's instructions (BBC Biochemical, Atlanta, GA). Tissue sections were examined under a regular microscope and photo images were taken using the NIS-Elements imaging software from Nikon Instruments Inc. (Melville, NY).

Statistical analyses

Statistical significance was determined using unpaired student *t*-test. A *P*<0.05 was considered significantly different. Values are expressed as means \pm SD.

Results

Establishment of tumor growth in the lung, liver, and kidneys by hydrodynamic cell delivery

A single colony of luciferase expression Renca^{Luc} cells was expanded and hydrodynamically injected into Balb/c mice (1×10^6 Renca^{Luc} cells/mouse). Tumor nodules in the lung, liver and kidneys were examined 18 days post cell injection. Photo images for the external appearance of the three organs show multiple tumor nodules in the lung and the liver, but absent in the kidneys (**Figure 1A**). However, H&E staining of tissue sections (**Figure 1B**) of the same organs show tumor growth in all three organs. These results confirm the effectiveness of the hydrodynamic procedure for establishment of tumor growth in the lung, liver and kidneys.

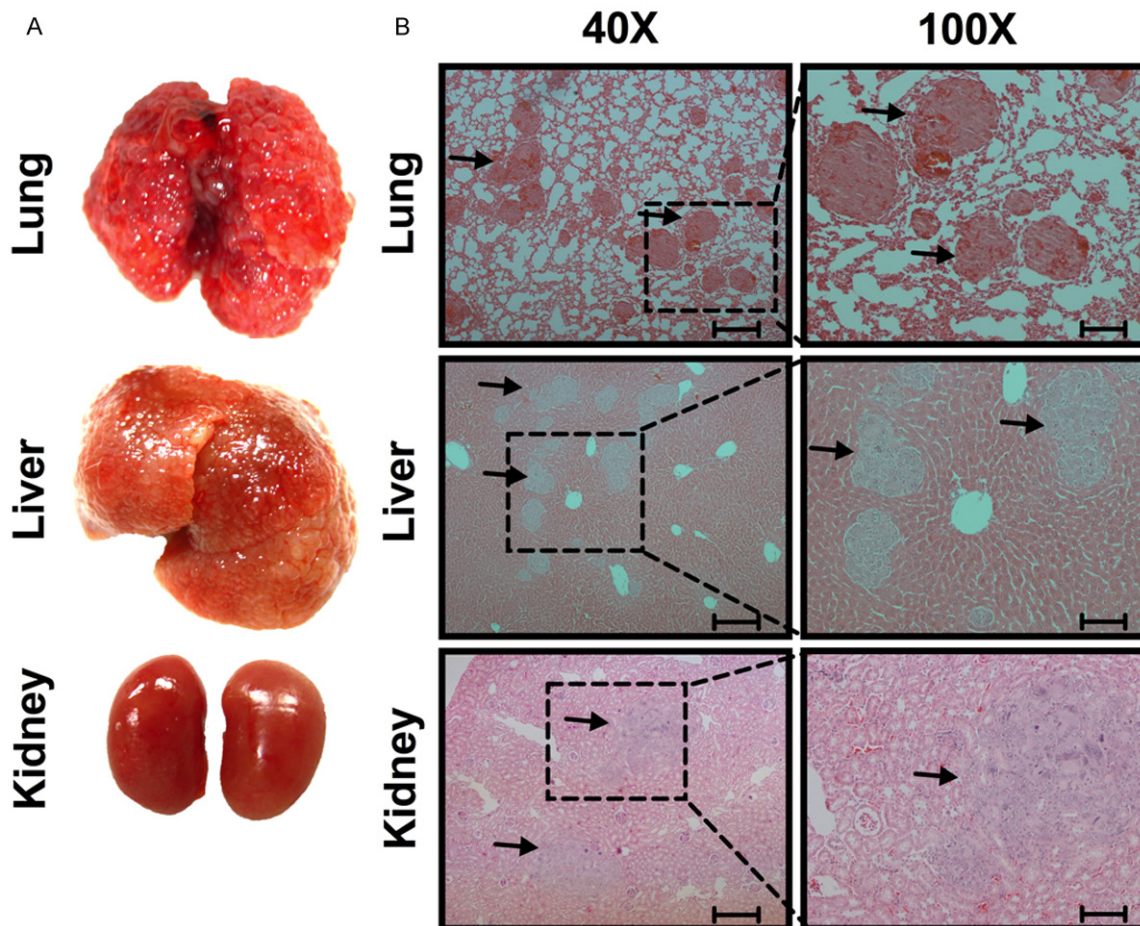


Figure 1. Establishment of tumor growth by hydrodynamic cell delivery. Balb/c mice were hydrodynamically injected with 1×10^6 Renca^{Luc} cells/mouse. Mice were euthanized 18 days after injection, and the lung, liver and kidneys were collected and examined. A. Representative images of tumor-bearing lung, liver and kidneys. B. H&E staining of tissue sections of the lung, liver, and kidneys. The structures indicated with arrows are tumor nodules. Scale bars represent 250 μ m (40 \times) and 100 μ m (100 \times).

Tumor cell distribution and characterization of tumor growth

More tumor nodules seen in the lung and liver, and less in the kidneys (**Figure 1A**) suggest a difference in tumor load among the organs. Such difference could be due to uneven delivery of tumor cells to the organs by tail vein hydrodynamic delivery, or to different growth rates of the tumor in different organs. To test these possibilities, Renca^{Luc} cells were hydrodynamically injected into mice and their tissue distribution was examined 6 h later before possible proliferation could take place. *In vivo* bioluminescence imaging shows the expression of luciferase in injected Renca^{Luc} cells 6 h post injection (**Figure 2A**). Animals were then sacrificed and internal organs collected for luciferase

assay. Quantification of luciferase activity in each of the three dissected organs shows that there are 24.5% and 11.4% of the injected cells distributed to the lung and liver (**Figure 2B**), respectively. Luciferase activity in the kidneys was below the detection limit of our luciferase assay, suggesting a minimal cell delivery for hydrodynamic injection to the kidneys. It appears that we lost about 65% of estimated luciferase activity based on values derived from the standard curve of luciferase activity as a function of Renca^{Luc} cell numbers. These results suggest that hydrodynamic injection created an uneven cell distribution among the three organs involved.

Similar experiments were performed to examine the tumor load in different organs as a func-

Environment affects tumor growth and response to treatment

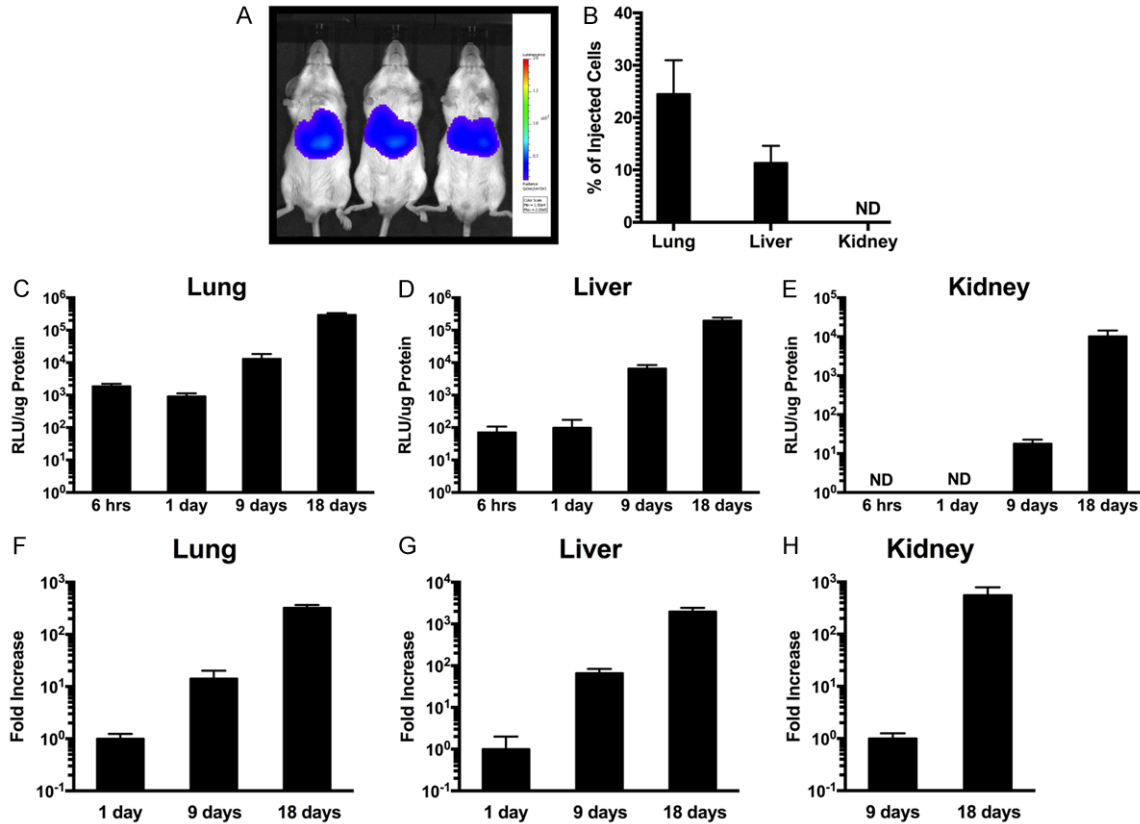


Figure 2. Renca^{Luc} cell distribution and characterization of tumor growth rates in different organs. Balb/c mice were hydrodynamically injected with 1×10^6 Renca^{Luc} cells/mouse. Mice were imaged using *in vivo* bioluminescence imaging at 6 h after injection. Different groups of mice were euthanized on 6 h, 1, 9, and 18 days, organs were collected and luciferase activity was determined. A. Ventral view of the *in vivo* bioluminescence image shows adequate light emitted from tumor cells 6 h after hydrodynamic cell injection. B. Organ distribution of Renca^{Luc} cells 6 h after hydrodynamic injection of tumor cells. C-E. Estimation of tumor burden in different organs at different time points judging from luciferase activity (RLU/ μ g of protein). F-H. Increase of tumor mass on days 9 and 18 in the lung and liver compared to that of day 1, and folds of increase of tumor burden in kidneys between days 9 and 18. Values represent mean \pm SD (n=3), * $P < 0.05$. ND: not detected.

tion of time. Results in **Figure 2C** show a slight decrease of the luciferase activity in the lung from 6 to 24 h, suggesting a loss of luciferase expression cells in this organ. However, luciferase activity increased from day 1 on. At the end of the 18-day experiment after cell injection, a similar level of tumor load was seen in the lung and liver with luciferase activity at approximately 10^5 RLU per microgram of proteins of the tissue homogenates (**Figure 2C** and **2D**). Interestingly, until day 9, luciferase activity in the kidneys was below our detection limit, indicating minimal tumor cell proliferation (**Figure 2E**).

Tumor growth rate in different organs was determined by the fold increase of luciferase activity for the lung (**Figure 2F**), liver (**Figure 2G**), and kidneys (**Figure 2H**). The number of

tumor cells in the lung increased 14 and 23 folds from days 1 to 9, and days 9 to 18, respectively. Similarly, the increase in the liver was 66 folds from days 1 to 9, and 30 folds from days 9 to 18. Compared to the lung and liver, tumors in the kidneys expanded 557 folds between days 9 and 18, suggesting that tumor growth in the kidneys was slow initially and expanded rapidly once reaching a threshold level.

Tumors growing in different organs respond to treatment differently

Two approaches were taken to examine how Renca^{Luc} cells seeded in the lung, liver and kidneys respond to treatment. The first approach employed 5-FU as an anticancer drug. Tumor-bearing mice were treated with 5-FU (20 mg/kg in 100 μ l, *i.p.*) every other day for 12 days start-

Environment affects tumor growth and response to treatment

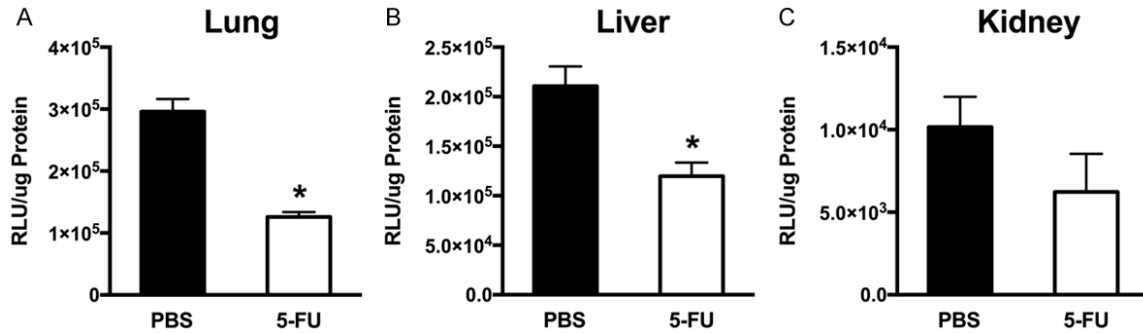


Figure 3. Different response of RCC tumors growing in different organs to 5-FU treatment. Balb/c mice were hydrodynamically injected with 1×10^6 Renca^{Luc} cells/mouse. Seven days after cell injection, mice were injected (*i.p.*) with 20 mg/kg of 5-FU every other day for a total of 6 times. Mice were euthanized on day 18 and organs were collected and assessed. A-C. Quantification of tumor burden in the lung, liver, and kidneys, respectively, determined by luciferase activity (RLU/ μ g of protein). Values represent mean \pm SD (n=4), *P<0.05.

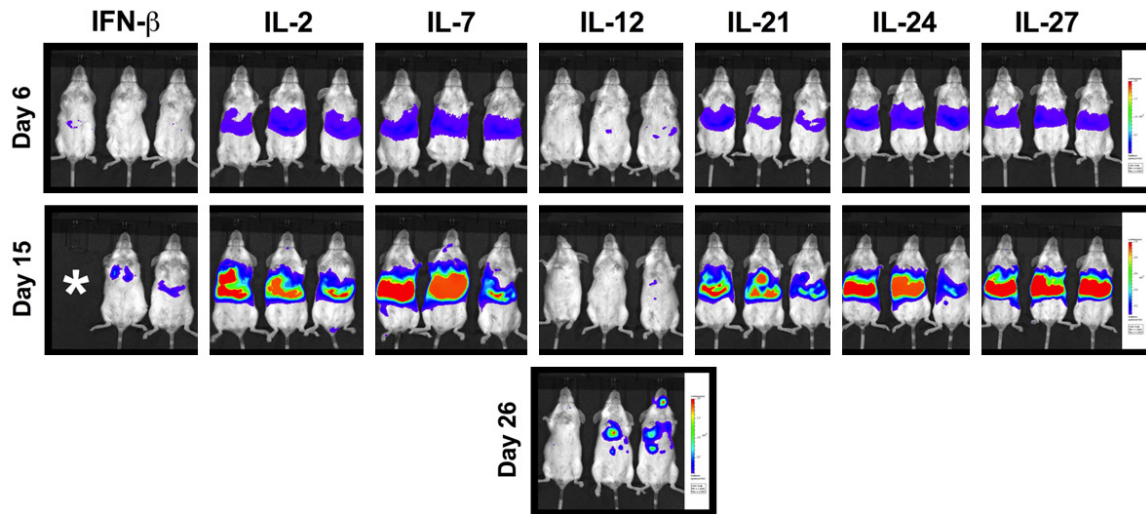


Figure 4. Assessment of antitumor activity of cytokine genes by hydrodynamic gene transfer. Balb/c mice were hydrodynamically injected with 1×10^6 Renca^{Luc} cells/mouse. Three days after tumor injection, tumor-bearing mice were hydrodynamically injected with cytokine gene-containing plasmid DNA (IFN- β : 10 μ g/mouse, IL-2: 2.5 μ g/mouse, others: 20 μ g/mouse). Mice were imaged using *in vivo* bioluminescence imaging on days 6 and 15 after tumor cell injection. *One mouse was lost in IFN- β group when performing bioluminescence imaging on day 15.

ing on day 7 post hydrodynamic cell delivery. The control animals received an injection of PBS, the carrier solution.

Results in **Figure 3** show 5-FU treatments suppressed tumor growth in the lung by 57.4%, compared to 43.1% in the liver and 38.6% in the kidneys. While significant antitumor activity was seen in the lung and liver, as quantified by luciferase activity, tumor nodules were seen in all three organs (data not shown). These results suggest that 5-FU has limited effectiveness in suppressing growth of Renca^{Luc} cells in mice.

The second approach employed was gene therapy using different cytokine genes. Cytokine

genes were chosen based on their unique functions, including cytotoxic activity against tumor cells (IFN- β and IL-24); activation of B cells (IL-21); activation of T cells and NK cells (IL-2, IL-7 and IFN- β); and activation of Th1 cells (IL-12 and IL-27) [17-23]. Three days after tumor cell injection, twenty-one tumor-bearing mice were randomly divided into seven groups, and each group received a hydrodynamic injection of pLIVE plasmid containing one of the cytokine genes (IL-2: 2.5 μ g/mouse, IFN- β : 10 μ g/mouse, others: 20 μ g/mouse). Tumor growth over time was monitored using *in vivo* bioluminescence imaging on days 6 and 15. Results show that both IFN- β and IL-12 suppressed tumor growth while others failed to show signifi-

Environment affects tumor growth and response to treatment

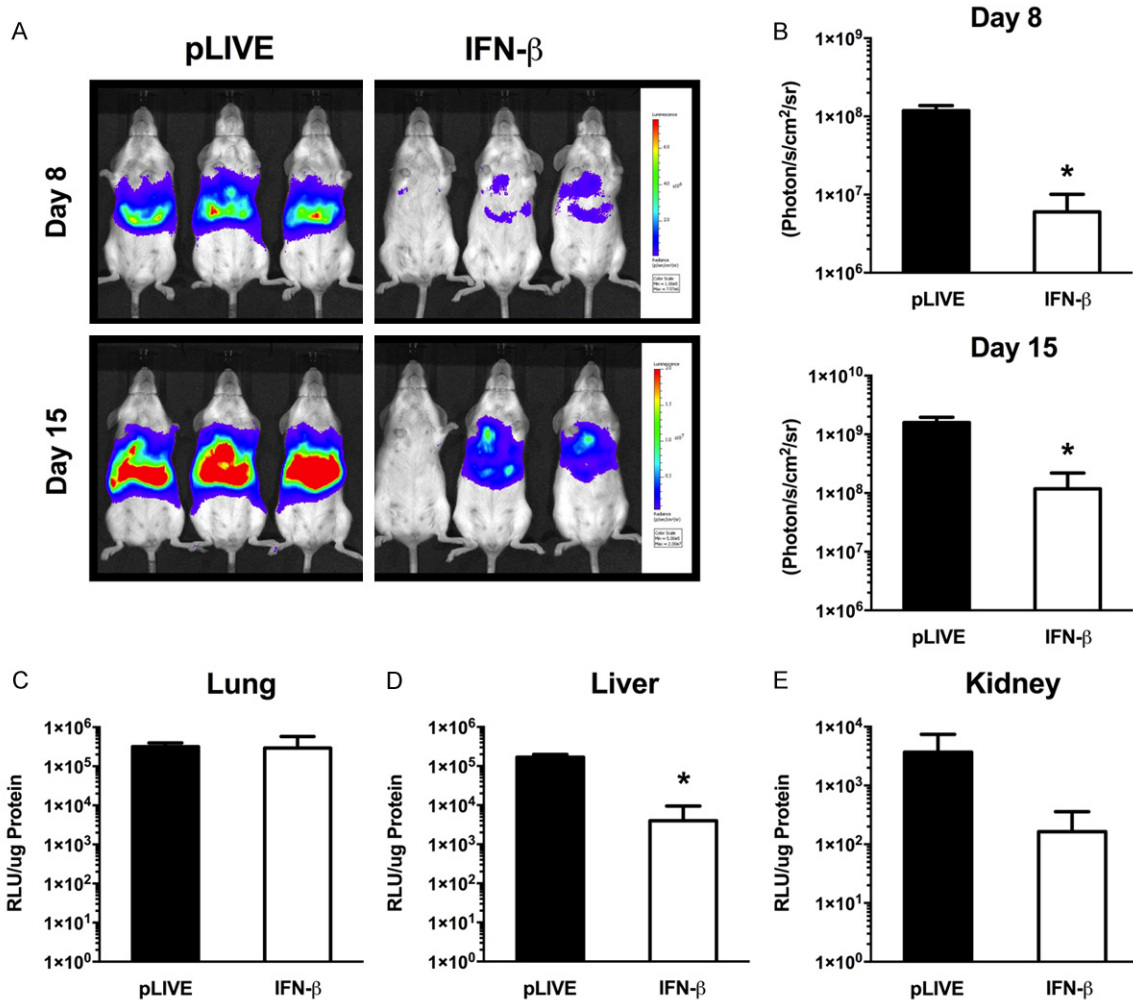


Figure 5. Quantitative assessment of the impact of IFN- β gene transfer on tumor growth. Balb/c mice were hydrodynamically injected with 1×10^6 Renca^{Luc} cells/mouse. Three days later, animals (3 mice/group) were hydrodynamically injected with empty plasmid (control) or plasmids carrying IFN- β gene. Mice were imaged using *in vivo* bioluminescence imaging on days 8 and 15. Mice were euthanized on day 18 after cell injection and organs collected for luciferase assay. A. *In vivo* bioluminescence images of the control and treated animals with hydrodynamic IFN- β gene transfer. B. Quantification of bioluminescence measurements for imaged areas of animals after 8 and 15 days of tumor injection, mean \pm SD (n=3), * P <0.05. C-E. Quantification of tumor burden in different organs of control and treated animals based on luciferase assay, mean \pm SD (n=3), * P <0.05.

cant antitumor effects (**Figure 4**). A single injection of IL-12 plasmid was sufficient to prolong animal survival to more than 32 days, compared to other animals that showed signs of morbidity on day 18.

The suppression effect of IFN- β gene therapy on multi-organ RCC model was further evaluated with a lower dose to avoid potential toxicity. On day 3 post tumor cell injection, 6 tumor-bearing mice were randomly divided into control and treated groups. The control group received a hydrodynamic injection of empty

pLIVE plasmid while the IFN- β treated group received pLIVE-IFN- β (4 μ g/mouse) plasmid DNA. *In vivo* bioluminescence imaging results on days 8 and 15 show that IFN- β significantly suppressed tumor growth compared to control (**Figure 5A** and **5B**). Results of luciferase activity assessment on tumor-bearing organs indicate that tumor suppression obtained by IFN- β was due to inhibition of tumor growth in the liver, but not in the lung (**Figure 5C** and **5D**). Suppression of tumor growth was also seen in the kidneys (**Figure 5E**). Images of collected organs (**Figure 6A**) exhibit that IFN- β was highly

Environment affects tumor growth and response to treatment

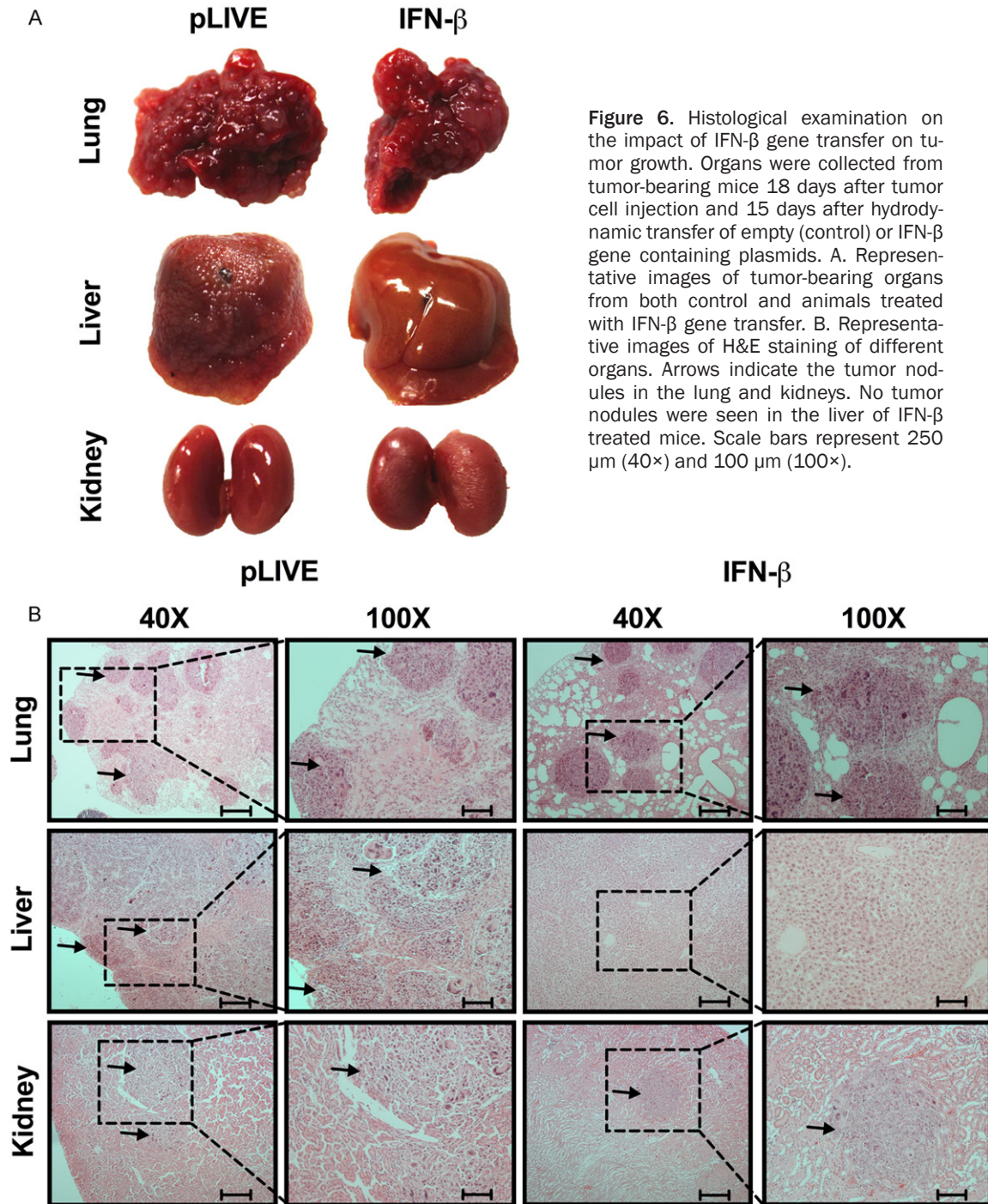


Figure 6. Histological examination on the impact of IFN- β gene transfer on tumor growth. Organs were collected from tumor-bearing mice 18 days after tumor cell injection and 15 days after hydrodynamic transfer of empty (control) or IFN- β gene containing plasmids. A. Representative images of tumor-bearing organs from both control and animals treated with IFN- β gene transfer. B. Representative images of H&E staining of different organs. Arrows indicate the tumor nodules in the lung and kidneys. No tumor nodules were seen in the liver of IFN- β treated mice. Scale bars represent 250 μ m (40 \times) and 100 μ m (100 \times).

effective in suppressing tumor growth in the liver, as observed by the absence of tumor nodules on the surface of this organ. There was no obvious difference in the tumor load in the lung between treated and control animals. Results from histological examination of these animals are in full agreement with these conclusions (Figure 6B). These results provide direct evidence in support that the same tumor growth

in different organs responds differently to the same treatment differently, indicating the importance of environment in determining the outcome of cancer treatment.

Discussion

A multi-organ RCC model for an accurate pre-clinical drug assessment is an unmet need.

Environment affects tumor growth and response to treatment

In the present work, we exploit hydrodynamic delivery strategy to simultaneously implant quantifiable Renca cells in the lung, liver, and kidneys. The mechanism underlying multi-organ cell delivery of hydrodynamic injection involves flow dynamics of injected solution determined by the vasculature of the inferior vena cava (IVC) [24]. When a large volume of Renca^{Luc} cell suspension equivalent to 9% of body weight is rapidly injected into a mouse tail vein, a cardiac congestion is generated as the volume exceeds the cardiac output, resulting in elevation of intravascular pressure in IVC. This pressure forces tumor cells to enter the liver and kidneys through hepatic and renal veins in retro grade, respectively. While some cells will remain in the liver and kidneys once they reach these organs, the significant majority of tumor cells will go through the heart and reach the lung when the heart regains its function and resumes the regular blood flow in time. Consequently, tumor cells are seeded in three organs with different environments that are critical in support of tumor growth.

Results in **Figure 2B** show that the lung received the highest number of cells from hydrodynamic injection, judging by the luciferase activity detected 6 h post injection representing 24.5% of injected dose. However, a significant drop in luciferase activity was seen at the time point of 1 day (**Figure 2C**), suggesting a loss of tumor cells in the lung compared to a sustained level of luciferase activity detected in the liver (**Figure 2D**). The luciferase activity in the kidneys (**Figure 2E**) was below detection limit during the same time period.

Tumor growth rates vary in different organs. Using luciferase activity 1 day after injection as a baseline, the calculated activity increased 14 folds in the lung, and 66 folds in the liver on day 9, respectively, with further increase to 322 folds in the lung and 1977 folds in the liver on day 18 (**Figure 2F** and **2G**). In the kidneys, tumor cells were below our detection limit at earlier time points but proliferated aggressively to 557 folds between days 9 to 18 post tumor injection, marking their growth rate the highest compared to those of the lung and liver for the same period (**Figure 2H**). It appears that the kidneys offer the best environment for Renca^{Luc} cells to grow, followed by the liver, with the lung being the most unfavorable among the three.

Considering the unique influence of each organ on the tumor growth, it is reasonable to expect that tumors' response to antitumor drugs would vary depending on the environment where the tumor cells grow. The results in **Figures 3-6** provide direct evidence in support of such a prediction. Treatment with 5-FU and by the gene therapy approach with IFN- β and IL-12 resulted in various responses. 5-FU chemotherapy and IFN- β gene therapy exhibited better antitumor activity in the liver. Tumor in the lung was sensitive to 5-FU but not to IFN- β gene therapy. Conversely, 5-FU and IFN- β monotherapies did not produce significant tumor inhibition in the kidneys.

A surprising observation in the study is that not all cytokines, even those belonging to the same family, possess similar effectiveness. For example, while IFN- β gene therapy show liver-specific tumor suppression, IL-12 gene therapy exerts a whole-body antitumor activity that significantly prolonged the survival time of tumor-bearing mice. While additional studies are needed, these results may suggest that difference between different cytokine gene therapy is due to various activities of the cytokines expressed in activating the different types of immune cells at the tumor sites.

In conclusion, a multi-organ tumor model of RCC was established using the hydrodynamic delivery technique. This model offers a precise preclinical evaluation of antitumor drugs targeting RCC. The model can also be utilized to study the interaction between tumor cells and the surrounding environment in different organs. Distinct differences in tumor growth and response to treatment in various organs as a result of environmental heterogeneity offer an opportunity to study the underlying mechanisms and to identify factors that play critical role in support tumor proliferation. Our findings emphasize the importance of considering the anatomical site of metastasis when deciding the use of a particular therapeutic regime. Also, this work suggests the need for a combination therapy to eradicate tumors in various organs.

Acknowledgements

This work was supported in part by NIH grant (R01EB007357). Yahya Alhamhoom is supported by a scholarship from the King Khalid University (Abha, Saudi Arabia).

Disclosure of conflict of interest

None.

Address correspondence to: Dr. Dexi Liu, Department of Pharmaceutical and Biomedical Sciences, College of Pharmacy, University of Georgia, Athens, GA 30602, USA. E-mail: dliu@uga.edu

References

[1] Siegel RL, Miller KD and Jemal A. Cancer statistics, 2016. *CA Cancer J Clin* 2016; 66: 7-30.

[2] Koul H, Huh JS, Rove KO, Crompton L, Koul S, Meacham RB and Kim FJ. Molecular aspects of renal cell carcinoma: a review. *Am J Cancer Res* 2011; 1: 240-254.

[3] Motzer RJ and Russo P. Systemic therapy for renal cell carcinoma. *J Urol* 2000; 163: 408-417.

[4] Kjaer M, Iversen P, Hvidt V, Bruun E, Skaarup P, Bech Hansen J and Frederiksen PL. A randomized trial of postoperative radiotherapy versus observation in stage II and III renal adenocarcinoma. A study by the copenhagen renal cancer study group. *Scand J Urol Nephrol* 1987; 21: 285-289.

[5] Kjaer M, Frederiksen PL and Engelholm SA. Postoperative radiotherapy in stage II and III renal adenocarcinoma. A randomized trial by the copenhagen renal cancer study group. *Int J Radiat Oncol Biol Phys* 1987; 13: 665-672.

[6] Cohen HT and McGovern FJ. Renal-cell carcinoma. *N Engl J Med* 2005; 353: 2477-2490.

[7] Thomas JS and Kabbinavar F. Metastatic clear cell renal cell carcinoma: a review of current therapies and novel immunotherapies. *Crit Rev Oncol Hematol* 2015; 96: 527-533.

[8] Fisher RI, Rosenberg SA and Fyfe G. Long-term survival update for high-dose recombinant interleukin-2 in patients with renal cell carcinoma. *Cancer J Sci Am* 2000; 6 Suppl 1: S55-57.

[9] McDermott DF, Regan MM, Clark JI, Flaherty LE, Weiss GR, Logan TF, Kirkwood JM, Gordon MS, Sosman JA, Ernstoff MS, Tretter CP, Urba WJ, Smith JW, Margolin KA, Mier JW, Gollub JA, Dutcher JP and Atkins MB. Randomized phase III trial of high-dose interleukin-2 versus subcutaneous interleukin-2 and interferon in patients with metastatic renal cell carcinoma. *J Clin Oncol* 2005; 23: 133-141.

[10] Hay M, Thomas DW, Craighead JL, Economides C and Rosenthal J. Clinical development success rates for investigational drugs. *Nat Biotechnol* 2014; 32: 40-51.

[11] Devaud C, Westwood JA, John LB, Flynn JK, Paquet-Fifield S, Duong CP, Yong CS, Pegram HJ, Stacker SA, Achen MG, Stewart TJ, Snyder LA, Teng MW, Smyth MJ, Darcy PK and Ker-

shaw MH. Tissues in different anatomical sites can sculpt and vary the tumor microenvironment to affect responses to therapy. *Mol Ther* 2014; 22: 18-27.

[12] Lundqvist A, Yokoyama H, Smith A, Berg M and Childs R. Bortezomib treatment and regulatory T-cell depletion enhance the antitumor effects of adoptively infused NK cells. *Blood* 2009; 113: 6120-6127.

[13] Capitanio U, Abdollah F, Matloob R, Salonia A, Suardi N, Briganti A, Carenzi C, Rigatti P, Montorsi F and Bertini R. Effect of number and location of distant metastases on renal cell carcinoma mortality in candidates for cytoreductive nephrectomy: implications for multimodal therapy. *Int J Urol* 2013; 20: 572-579.

[14] Li J, Yao Q and Liu D. Hydrodynamic cell delivery for simultaneous establishment of tumor growth in mouse lung, liver and kidney. *Cancer Biol Ther* 2011; 12: 737-741.

[15] Liu F, Song Y and Liu D. Hydrodynamics-based transfection in animals by systemic administration of plasmid DNA. *Gene Ther* 1999; 6: 1258-1266.

[16] Zhang G, Budker V and Wolff JA. High levels of foreign gene expression in hepatocytes after tail vein injections of naked plasmid DNA. *Hum Gene Ther* 1999; 10: 1735-1737.

[17] Chawla-Sarkar M, Leaman DW and Borden EC. Preferential induction of apoptosis by interferon (IFN)-beta compared with IFN-alpha2: correlation with TRAIL/Apo2L induction in melanoma cell lines. *Clin Cancer Res* 2001; 7: 1821-1831.

[18] Park MA, Walker T, Martin AP, Allegood J, Vozhilla N, Emdad L, Sarkar D, Rahmani M, Graf M, Yacoub A, Koumenis C, Spiegel S, Curriel DT, Voelkel-Johnson C, Grant S, Fisher PB and Dent P. MDA-7/IL-24-induced cell killing in malignant renal carcinoma cells occurs by a ceramide/CD95/PERK-dependent mechanism. *Mol Cancer Ther* 2009; 8: 1280-1291.

[19] Kuchen S, Robbins R, Sims GP, Sheng C, Phillips TM, Lipsky PE and Ettinger R. Essential role of IL-21 in B cell activation, expansion, and plasma cell generation during CD4+ T cell-B cell collaboration. *J Immunol* 2007; 179: 5886-5896.

[20] Liao W, Lin JX and Leonard WJ. IL-2 family cytokines: new insights into the complex roles of IL-2 as a broad regulator of T helper cell differentiation. *Curr Opin Immunol* 2011; 23: 598-604.

[21] Swann JB, Hayakawa Y, Zerafa N, Sheehan KC, Scott B, Schreiber RD, Hertzog P and Smyth MJ. Type I IFN contributes to NK cell homeostasis, activation, and antitumor function. *J Immunol* 2007; 178: 7540-7549.

[22] Hsieh CS, Macatonia SE, Tripp CS, Wolf SF, O'Garra A and Murphy KM. Development of

Environment affects tumor growth and response to treatment

- TH1 CD4+ T cells through IL-12 produced by Listeria-induced macrophages. *Science* 1993; 260: 547-549.
- [23] Pflanz S, Timans JC, Cheung J, Rosales R, Kanzler H, Gilbert J, Hibbert L, Churakova T, Travis M, Vaisberg E, Blumenschein WM, Mattson JD, Wagner JL, To W, Zurawski S, McClanahan TK, Gorman DM, Bazan JF, de Waal Malefyt R, Rennick D and Kastelein RA. IL-27, a heterodimeric cytokine composed of EB13 and p28 protein, induces proliferation of naive CD4+ T cells. *Immunity* 2002; 16: 779-790.
- [24] Kanefuji T, Yokoo T, Suda T, Abe H, Kamimura K and Liu D. Hemodynamics of a hydrodynamic injection. *Mol Ther Methods Clin Dev* 2014; 1: 14029.